

PACS: 74.20.-z

UDC: 538.945

Structural and electroresistive properties of layered compounds based on the 1-2-3 HTSC system and transition metal dichalcogenides under extreme external influences (review)

A.L. Solovyov^{1,2}, N.R. Vovk^{2,3}

1 B.I. Verkin Institute for Low Temperature Physics and Engineering of National Academy of Science of Ukraine, 47 Nauki ave., 61103 Kharkov, Ukraine

2 V.N. Karazin Kharkiv National University, Svobody Sq. 4, Kharkiv 61022, Ukraine.

*3 IFIMUP, Departamento de Fisica, Universidade de Porto, 4169-007 Porto, Portugal.
nikolayvovk94@gmail.com*

ORCID: 0000-0001-8858-1177, 0000-0001-8697-4452

DOI: 10.26565/2222-5617-2020-33-03

The problem of the influence of extreme external influences (high pressure, sharp temperature drops, structural relaxation, and strong magnetic fields) on various mechanisms of electric transport of HTSC compounds $\text{Re}_1\text{Ba}_2\text{Cu}_3\text{O}_{7-\delta}$ (Re = Y or another rare-earth ion) and dichalcogenides of transition metals are considered. The features of the crystal structure and the effect of structural defects of various morphologies on the electrical conductivity of these compounds in the normal, pseudogap, and superconducting states are discussed. A review of the experimental data obtained in the study of the effect of high hydrostatic pressure and other extreme effects on various mechanisms of electric transport of $\text{Re}_1\text{Ba}_2\text{Cu}_3\text{O}_{7-\delta}$ compounds of various compositions and transition metal dichalcogenides of various technological backgrounds is carried out. Various theoretical models devoted to the effect of high pressure on the electrical conductivity of HTSC compounds of the 1-2-3 system and transition metal dichalcogenides are discussed, and a comprehensive comparative analysis of their magnetoresistive characteristics under extreme external influences is performed. In particular, it was shown, that the relatively weak effect of pressure on the T_c value of optimally doped samples can be explained within the framework of a model assuming the presence of a Van Hove singularity in the spectrum of charge carriers which is characteristic of strongly coupled lattices. This is confirmed by the observation similar features of the behavior of the baric derivatives dT_c/dP depending on the change composition in NbSe_2 single crystals, which also belong to systems of two-dimensional lattices and have a similar anisotropy parameter. Nevertheless, it is still possible to formulate a number of questions that have not yet found a final experimental and theoretical solution. Namely, what is the role of the crystal lattice and structural defects and, in particular, twinning planes? What is the reason for the broadening of the resistive transitions of HTSC compounds into the superconducting state under pressure, and what is the relationship between this broadening and charge transfer and the nature of the redistribution of the vacancy subsystem? What is the role of phase separation in the implementation of different modes of longitudinal and transverse transport? Obviously, more research, both experimental and theoretical, is needed to answer these questions.

Keywords: High-temperature superconductivity (HTSC), external influences, mechanisms of electric transport.

Структурні та електрорезистивні властивості шаруватих сполук на основі 1-2-3 ВТНП системи та дихалкогенідів перехідних металів при екстремальних зовнішніх впливах (огляд)

А.Л. Соловйов^{1,2}, М.Р. Вовк^{2,3}

1 Фізико-технічний інститут низьких температур ім. Б.І. Веркіна НАН України, пр. Науки 47, Харків, 61103, Україна

2 Харківський національний університет імені В.Н. Каразіна, м. Свободи 4, 61022, Харків, Україна

3 IFIMUP, Departamento de Fisica, Universidade de Porto, 4169-007 Porto, Portugal.

Розглянуто проблему впливу екстремальних зовнішніх факторів (високого тиску, стрибкоподібного зміни температури, структурної релаксації і високих магнітних полів) на різні механізми електротранспорту ВТНП сполук $\text{Re}_1\text{Ba}_2\text{Cu}_3\text{O}_{7-\delta}$ (Re = Y або інший рідкоземельні іон) і дихалкогенідів перехідних металів. Обговорюються особливості кристалічної структури та впливу структурних дефектів різної морфології на електропровідність цих сполук в нормальному, псевдощільному, і надпровідному станах. Проведено огляд експериментальних даних, отриманих при дослідженнях впливу високого гідростатичного тиску і інших екстремальних впливів на різні механізми електротранспорту з'єднань $\text{Re}_1\text{Ba}_2\text{Cu}_3\text{O}_{7-\delta}$ різного складу і дихалкогенідів перехідних металів різної технологічної передісторії. Обговорюються різні теоретичні моделі

присвячені питанню впливу високого тиску на електропровідність ВТНП сполук системи 1-2-3 і діхалькогенідів перехідних металів, а також проведено комплексний порівняльний аналіз їх магніторезистивних характеристик в умовах екстремальних зовнішніх факторів. Зокрема, було показано, що відносно слабкий вплив тиску на значення T_c оптимально легованих зразків можна пояснити в рамках моделі, що передбачає наявність сингулярності Ван Хофа в спектрі носіїв заряду, що характерно для сильно пов'язаних решіток. Це підтверджується спостереженням подібних особливостей поведінки барических похідних dT_c/dP в залежності від зміни складу в монокристалах $NbSe_2$, які також відносяться до систем двовимірних решіток і мають аналогічний параметр анізотропії. Проте, все ще можна сформулювати ряд питань, які ще не знайшли остаточного експериментального і теоретичного рішення. А саме, яка роль кристалічної решітки і структурних дефектів і, зокрема, площин дублювання? У чому причина розширення резистивних переходів ВТНП-з'єднань в надпровідний стан під тиском і який зв'язок між цим розширенням, перенесенням заряду і характером перерозподілу вакансійних підсистеми? Яка роль фазового розділення в реалізації різних видів подовжнього і поперечного переносу? Очевидно, що для відповіді на ці питання необхідні додаткові дослідження, як експериментальні, так і теоретичні.

Ключові слова: Високотемпературна надпровідність (ВТНП), вплив зовнішніх факторів, механізми електротранспорту.

Структурные и электрорезистивные свойства слоистых соединений на основе 1-2-3 ВТСП систем и дихалькогенидов переходных металлов при экстремальных внешних воздействиях (обзор)

А.Л. Соловьёв^{1,2}, Н.Р. Вовк^{2,3}

1 Физико-технический институт низких температур им. Б. Веркина НАН Украины, пр-т Науки 47, 61103 Харьков, Украина

2 Харьковський національний університет імені В.Н. Каразіна, м. Свободи 4, 61022, Харьков, Украина

3 IFIMUP, Departamento de Fisica, Universidade de Porto, 4169-007 Porto, Portugal.

Рассмотрена проблема влияния экстремальных внешних воздействий (высокого давления, скачкообразного изменения температуры, структурной релаксации и высоких магнитных полей) на различные механизмы электротранспорта ВТСП соединений $Re_1Ba_2Cu_3O_{7-\delta}$ ($Re=Y$ или другой редкоземельный ион) и дихалькогенидов переходных металлов. Обсуждаются особенности кристаллической структуры и влияния структурных дефектов различной морфологии на электропроводность этих соединений в нормальном, псевдощелевом, и сверхпроводящем состоянии. Проведен обзор экспериментальных данных, полученных при исследованиях влияния высокого гидростатического давления и других экстремальных воздействий на различные механизмы электротранспорта соединений $Re_1Ba_2Cu_3O_{7-\delta}$ разного состава и дихалькогенидов переходных металлов различной технологической предьстории. Обсуждаются различные теоретические модели посвященные вопросу влияния высокого давления на электропроводимость ВТСП соединений системы 1-2-3 и дихалькогенидов переходных металлов, а также проведен комплексный сравнительный анализ их магніторезистивных характеристик в условиях экстремальных внешних воздействий. В частности, было показано, что относительно слабое влияние давления на значение T_c оптимально легированных образцов можно объяснить в рамках модели, предполагающей наличие сингулярности Ван Хофа в спектре носителей заряда, что характерно для сильно связанных решеток. Это подтверждается наблюдением схожих особенностей поведения барических производных dT_c/dP в зависимости от изменения состава в монокристаллах $NbSe_2$, которые также относятся к системам двумерных решеток и имеют аналогичный параметр анизотропии. Тем не менее, всё ещё можно сформулировать ряд вопросов, которые еще не нашли окончательного экспериментального и теоретического решения. А именно, какова роль кристаллической решетки и структурных дефектов и, в частности, плоскостей дублювания? В чем причина уширения резистивных переходов ВТСП-соединений в сверхпроводящем состоянии под давлением и какова связь между этим уширением, переносом заряда и характером перераспределения вакансионной подсистемы? Какова роль фазового разделения в реализации различных видов продольного и поперечного переноса? Очевидно, что для ответа на эти вопросы необходимы дополнительные исследования, как экспериментальные, так и теоретические.

Ключевые слова: Високотемпературная сверхпроводимость (ВТСП), влияние внешних воздействий, механизмы электротранспорта.

Introduction

Anisotropic quasi-two-dimensional conducting compounds represent a large class of solids with unique physical properties. These compounds include transition metal dichalcogenides (TMDs) [1] and high-temperature superconductors (HTSCs or cuprates) [2,3 and references there in], the best-known representatives of which are layered single crystals of the 1-2-3 system - $REBa_2Cu_3O_{7-\delta}$ ($RE = Y$ or another rare-earth ion) and $NbSe_2$. It should be noted that a new surge of interest in the study of layered crystals arose precisely after the discovery in 1986 of high-

temperature superconductivity in nonstoichiometric oxides with pronounced anisotropy of physical characteristics, the main structural unit of which are the CuO_2 planes separated by atoms of rare-earth and other elements, depending on specific composition [2]. Revealing similar physical characteristics and distinctive features between low-temperature and high-temperature superconductors associated with the crystal structure and the mechanism of superconductivity is an urgent problem in solid-state physics.

According to the modern concepts, the main difficulty lies in understanding the unusual properties of HTSC compounds in the normal (non-superconducting) state [4-7]. In the absence of a microscopic theory of high-temperature superconductivity, experimental methods are of particular importance, which make it possible to reveal the physical parameters that most significantly affect the critical characteristics of HTSC compounds [8]. This, in turn, makes it possible not only to check the numerous theoretical models that exist at this time but also to determine empirical ways to increase the conducting characteristics of HTSCs. Studies of the metallic state of matter under extreme conditions are of great importance for solid-state physics. These methods include the use of high pressures [9,10], low temperatures [8] and high magnetic fields [11,12]. Such experiments can significantly expand the understanding of physical phenomena occurring in two subsystems: a crystal lattice and an ensemble of valence electrons, and also make it possible to find out how various electrical and superconducting properties of solids change. An important role in this case is played by varying the composition of the compounds under study, including the complete or partial replacement of components by their isoelectronic analogs. For example, in samples of the 1-2-3 HTSC system that are nonstoichiometric in oxygen composition, a rare-earth ion can serve as a sensor sensitive to the local symmetry of its environment and the distribution of the charge density, since its change affects the crystal field, which forms the electronic structure of such an ion.

Of particular interest, in this aspect, are studies of the effect of high pressures [9,10] (and references there in) on the physical properties of layered conducting compounds based on the above-mentioned transition metal dichalcogenides (TMD) [1] and HTSCs [2,3]. These compounds are currently receiving widespread attention due to a number of their exceptional properties. These include, first of all, the strong anisotropy of mechanical and electronic characteristics [13], due to the specificity of the crystal structure. Due to their anisotropy, such crystals offer the opportunity to study the most exciting effects of solid-state physics in their two-dimensional or nearly two-dimensional manifestation [14]. It should also be noted that the anisotropy of layered compounds can be significantly enhanced by the introduction of foreign atoms or molecules into the interlayer space (intercalation process) [15], which significantly expands the range of issues under study.

For instance, the ability of transition metal dichalcogenides to intercalate is associated with hopes for the realization of high-temperature superconductivity in sandwich-type structures with an exciton mechanism proposed by Ginzburg [16]. Besides, in dichalcogenides of transition metals, the coexistence of a structural transition

to the state of a charge density wave [CDW] [12] and a superconducting transition is observed, which is the subject of intensive theoretical and experimental studies.

Despite the significant progress achieved to date in understanding the mechanisms of the influence of the structural composition and high pressure on the electrical transport characteristics of the above-mentioned layered conductors, a number of issues in this area still remain completely unclear. These issues include the effect of pressure on the metal-insulator transition and the pseudogap state, charge transfer and the nature of the redistribution of the vacancy oxygen subsystem, broadening of the resistive transition to the normal state, and some others. Taking into account the above, in this review, we study each of the listed issues and analyze the results obtained, taking into account the generalization of the authors' works, as well as the experimental and theoretical material accumulated in the literature. We also attempted to briefly analyze the current state of the available theoretical and experimental results devoted to this problem and also highlight the main issues that have not found their theoretical and experimental solution.

1. Features of the unit cell and structural defects of HTSC compounds $\text{YBa}_2\text{Cu}_3\text{O}_{7-\delta}$

1.1. Crystal structure. The structure and properties of $\text{YBa}_2\text{Cu}_3\text{O}_{7-\delta}$ are directly related to the oxygen index ($7-\delta$), which characterizes the content of oxygen vacancies. It was established by X-ray and neutron diffraction [17] that within the limits of the oxygen stoichiometry of $\text{YBa}_2\text{Cu}_3\text{O}_{7-\delta}$ there are two phases [18,19]. Fig. 1 shows the unit cells for compositions with the minimum and maximum oxygen content ($\delta = 1$ and $\delta = 0$). The unit cell of $\text{YBa}_2\text{Cu}_3\text{O}_7$ is rhombic (Pmmm), and the unit cell of $\text{YBa}_2\text{Cu}_3\text{O}_6$ is tetragonal (P4 / mmm).

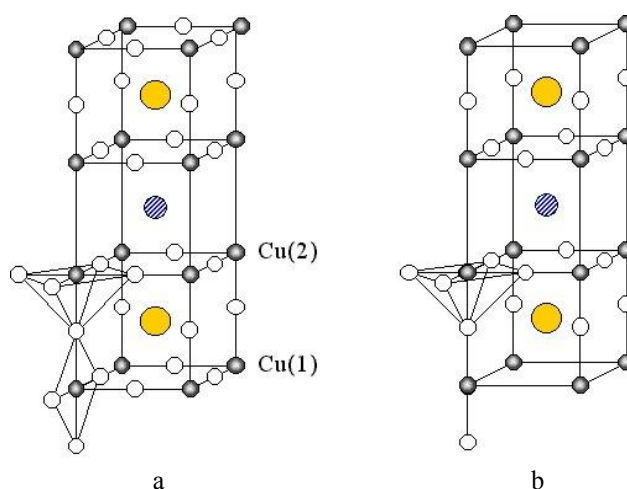


Fig. 1. The crystal lattice of the $\text{YBa}_2\text{Cu}_3\text{O}_{7-\delta}$ compound, according to [17].

In both cases, the structure is a derivative of the perovskite structure with the period c tripled due to the ordering of the cations according to the Ba-Y-Ba type. Two-thirds of the copper atoms (Cu (2)) are in tetragonal pyramidal coordination ($4 + 1$) of oxygen atoms, the latter being displaced from the basal plane of the pyramids by approximately 0.3 \AA along the c axis. One-third of copper atoms (Cu (1)) are located in the basal planes and have variable coordination for oxygen. In the $\text{YBa}_2\text{Cu}_3\text{O}_7$ (Fig. 1a) structure (the Cu (1) coordination number is 4), linear chains can be distinguished, formed by flat Cu (1) O4 squares elongated along the b axis. In the case of $\text{YBa}_2\text{Cu}_3\text{O}_6$ (Fig. 1b), oxygen atoms are entirely absent in the basal planes, and Cu (1) atoms have an oxygen coordination number equal to two. Thus, the occupancy of oxygen positions in the basal planes determines the oxygen nonstoichiometry of $\text{YBa}_2\text{Cu}_3\text{O}_{7-\delta}$ [18,19].

1.2. Structural defects in the compounds of the 1-2-3 system. In pure $\text{YBa}_2\text{Cu}_3\text{O}_{7-\delta}$ single crystals, depending on the oxygen deficiency and the synthesis technology, the following structural defects are observed: point defects such as oxygen vacancies that form in the CuO_2 planes, planar defects of the (001) type, twin boundaries, dislocations, and the so-called $2\sqrt{2} \times 2\sqrt{2}$ structures [20] observed at oxygen deficiency $\delta = 6.8 - 6.9$.

Plane defects are twinning planes, which are formed during the "tetra-ortho" transition and minimize the elastic energy of the crystal. Twin boundaries are planes with a tetragonal structure as a result of the presence of layers containing oxygen vacancies located along the twin boundary [20, 21]. Electron microscopic studies have shown [18,19,21] that at the initial stage of the tetra-ortho transition, domain nuclei are formed, in which two families of coherent interfaces (110) and ($\bar{1}\bar{1}0$) are formed. This may be the reason for the formation of a "tweed" type structure when close micro twins overlap. The period of such a structure depends on the oxygen content and can be stimulated by doping with a trivalent metal, in particular, aluminium [21, 22]. At the initial stage of the formation of microdomains, the formation of twin boundaries (TBs) occurs through the process of diffusion of structural vacancies in the CuO_2 layers. TB propagation occurs due to the movement of stress-controlled twin dislocations.

Linear defects (dislocations) are more likely to be characteristic of epitaxial films and textured samples. The source of this type of defects can be misfit dislocations generated by the film-substrate interface in film samples, and misfit dislocations generated at the $\text{YBa}_2\text{Cu}_3\text{O}_{7-\delta}$ and $\text{YBa}_2\text{Cu}_3\text{O}_5$ interface in textured fused samples. The dislocation density in films can reach values of about $1.4 \cdot 10^8 / \text{cm}^2$ [23].

A high dislocation density in $\text{YBa}_2\text{Cu}_3\text{O}_{7-\delta}$ single crystals can be obtained during crystal growth in the course

of the peritectic reaction [24], which is probably due to the presence of small inclusions of the $\text{YBa}_2\text{Cu}_3\text{O}_5$ phase. In crystals grown by the solution-melt method, the dislocation density is about $5 \cdot 10^3 / \text{cm}^2$ [25]. Note that the dislocation density can be increased by thermomechanical processing of materials [26].

Point defects (oxygen vacancies) are present in all $\text{YBa}_2\text{Cu}_3\text{O}_{7-\delta}$ samples, which is associated with the nonstoichiometric oxygen content. In this case, the filling factor is close to unity for all oxygen positions, with the exception of CuO (1) (refer to Fig. 1). Depending on the oxygen content, the formation of superstructures is possible with a periodic distribution of oxygen vacancies. The density of oxygen vacancies is relatively high, and at $\delta = 0.03$ it is about $10^{26} / \text{m}^3$.

There are also reports in the literature on a systematic copper deficit in the CuO_2 planes, which can reach values of 0.09 in compounds [27]. Point defects can also be produced by alloying. As a rule, alloying elements (except for rare earth elements and Sr) are incorporated into the Cu (1) position [28]. Ions of rare earth elements and K replace yttrium atoms, and Sr is incorporated into the positions of Ba atoms.

Additional defects can be created by irradiation [29,30]. Depending on the type of particles and their energy, both point and linear defects (tracks of heavy particles with high energy) can be created [31].

1.3. Influence of structural defects on electroresistive properties. The transport properties of HTSC materials substantially depend on the defectiveness of the structure and, in particular, on the oxygen content [32] and impurities [33, 34]. The specific electrical resistivity of $\text{YBa}_2\text{Cu}_3\text{O}_{7-\delta}$ single crystals with an oxygen content close to stoichiometric ($\delta \sim 0$) at room temperature is $\rho_{ab} = 200 \mu\text{Ohm} \cdot \text{cm}$ in the ab - plane and $\rho_c = 10 \text{ m}\Omega \cdot \text{cm}$ along the c axis [35]. In perfect single crystals, the electrical conductivity is quasi-metallic in all crystallographic directions [35–37]. However, even an insignificant deviation from stoichiometry, $\delta \leq 0.1$, leads to a quasi-semiconductor dependence $\rho_c(T)$, while maintaining the quasi-metallic character of the $\rho_{ab}(T)$ dependence. A further decrease in the oxygen content leads to a decrease in the density of charge carriers, thermal and electrical conductivity of the superconductor $\text{YBa}_2\text{Cu}_3\text{O}_{7-\delta}$, and with an oxygen deficit of $\delta \geq 0.6$, a metal-insulator transition is observed [37]. Doping $\text{YBa}_2\text{Cu}_3\text{O}_{7-\delta}$ single crystals with metal elements, except for the cases specified above, leads to the substitution of copper atoms in the CuO_2 planes. At the same time, data on the degree of influence of such a replacement are largely contradictory. For example, in [38], it is reported that, according to the data of different authors, the growth of ρ_{ab} in $\text{YBa}_2\text{Cu}_{3-z}\text{Al}_z\text{O}_7$ crystals at $z = 0.1$ can be less than 10%,

or can double at the same Al concentration. The reason for this discrepancy is probably the inhomogeneous distribution of Al over the volume of the crystals since when single crystals are grown in corundum crucibles, the introduction of Al occurs in an uncontrolled manner. In particular, broad transitions to the superconducting state $\Delta T_c \approx 2$ K indicate an inhomogeneous distribution of Al. There is also a significant scatter in the parameters of the superconducting state. Doping of $\text{YBa}_2\text{Cu}_3\text{O}_{7-\delta}$ with the substitution of rare-earth ions for yttrium practically does not change the transport characteristics of the normal and superconducting states [31, 36]. The exception is the replacement of yttrium atoms with praseodymium. In the concentration range $y \leq 0.05$, the charge carrier concentration and ρ_{ab} in the $\text{Y}_{1-y}\text{Pr}_y\text{Ba}_2\text{Cu}_3\text{O}_{7-\delta}$ superconductor weakly depend on the Pr concentration [39]. At $y \approx 0.5$, a sharp decrease in the concentration of charge carriers is observed, and at $y > 0.5$, the dependence $\rho(T)$ is observed, which is characteristic of semiconductors [39, 40].

As already noted, $\text{YBa}_2\text{Cu}_3\text{O}_{7-\delta}$ single crystals have plane defects - twin boundaries. The influence of these defects on the transport properties in the normal state was studied in [41], in which it was shown that twins are effective scattering centers of charge carriers. According to [41], the mean free path of electrons in single crystals is estimated to be 0.1 μm , which is an order of magnitude less than the intertwining distance. Therefore, the maximum increase in electrical resistance due to scattering can be 10%. A similar increase in resistance was observed when the current flowed across the TBs, compared with the resistance when the current flowed, along with the TBs [42].

1.4. Paraconductivity and the Aslamazov-Larkin theory. As is known from the literature [43], below a particular characteristic temperature T^* , the temperature dependences of the electrical resistivity in the basal plane $\rho_{ab}(T)$ of HTSC compounds deviate down from linear behavior in the normal state above T^* . This is due to the appearance of excess conductivity $\Delta\sigma$, the temperature dependence of which is given by the formula:

$$\Delta\sigma = \sigma - \sigma_0, \quad (1)$$

where $\sigma_0 = \rho_0^{-1} = (A + BT)^{-1}$ is the conductivity determined by interpolation of the linear section observed in the high-temperature measurement region to the zero-temperature value, and $\sigma = \rho^{-1}$ is the experimentally measured value of conductivity at $T < T^*$. It is known that near T_c the excess conductivity is most likely due to the processes of fluctuation pairing of charge carriers and can be described by the power dependence obtained in the theoretical

Lawrence-Doniach model [43], which assumes the presence of a very smooth crossover from two-dimensional to three-dimensional fluctuation conductivity with decreasing temperature:

$$\Delta\sigma = \left[\frac{e^2}{16\hbar d} \right] \varepsilon^{-1} \left\{ 1 + J\varepsilon^{-1} \right\}^{-1/2}, \quad (2)$$

where $\varepsilon = (T - T_c^{\text{mf}}) / T_c^{\text{mf}}$ is the reduced temperature. Accordingly, T_c^{mf} is the critical temperature in the mean-field approximation; $J = (2\xi_c(0)/d)^2$ is the constant of interplanar pairing; ξ_c is the coherence length along the c axis and d is the thickness of the two-dimensional layer. In HTSCs two limiting situations are possible. Near T_c , where $\xi_c \gg d$, the interaction between fluctuation Cooper pairs is realized in the entire volume of the superconductor, which corresponds to the three-dimensional (3D) case. Far above T_c , where $\xi_c \ll d$, interaction is possible only in the conducting CuO_2 planes, thus forming 2D fluctuation conductivity. Consequently, in both limiting cases expression (2) is transformed into the well-known relations for the two-dimensional and three-dimensional cases of the Aslamazov-Larkin (AL) theory [45]:

$$\Delta\sigma_{2D} = \frac{e^2}{16\hbar d} \varepsilon^{-1}, \quad (3)$$

$$\Delta\sigma_{3D} = \frac{e^2}{32\hbar\xi_c(0)} \varepsilon^{-1/2}, \quad (4)$$

In the case of comparison with experimental data, it is crucial to accurately determine the value of T_c^{mf} , which significantly affects the slope of the dependences $\Delta\sigma(\varepsilon)$. Usually, when compared with experimental data, $\xi_c(0)$ and T_c^{mf} in equations (2-4) are adjustable parameters [46], while $d = 11.7 \text{ \AA}$ is the size of the YBCO unit cell along the c axis [28]. However, when using such a technique, as a rule, there are significant quantitative discrepancies between theory and experiment. This, in turn, necessitates the use of a scaling factor, the so-called C-factor, as an additional adjustable parameter, which makes it possible to combine experimental data with calculated ones and, thus, take into account the possible inhomogeneity of the spreading of the transport current for each specific sample [47].

An important question is also to what temperature the dependence $\Delta\sigma(T)$ can be described within the framework of the fluctuation theory, since, according to modern concepts, the excess conductivity at temperatures sufficiently far from the critical temperature $T \gg T_c$ is a consequence of the manifestation of the so-called "pseudogap anomaly". Earlier it was experimentally found

[36,46] that with a sufficiently large increase in temperature above T_c , the fluctuation conductivity decreases faster than theory predicts. It was assumed that the reason for this lies in the underestimation of the contribution of short-wave fluctuations of the order parameter, while it increases with increasing temperature. In the works of Varlamov et al. [48, 49], a microscopic calculation of $\Delta\sigma(T)$ was carried out, taking into account all components of the order parameter. The comparison of experimental data with theory [48, 49] was carried out, in particular, in [3,50]. In this case, a good agreement with the theory was obtained up to temperatures near $T \approx 1.35 T_c$. With a further increase in temperature, it turned out again that $\Delta\sigma(T)$ decrease faster than it follows from the theory [48, 49]. Apparently, it is in this temperature range that a transition to the pseudogap regime occurs [3,50], which we will consider in more detail in the next section.

2. Phase diagram and the influence of extreme external influences on the phase state of HTSC compounds.

2.1. Features of the generalized HTSC phase diagram.

In the parent state all HTSCs are Mott insulators with a long-range antiferromagnetic (AF) order (Fig. 2). When holes appear in HTSC upon doping, the long-range AF order quickly disappears and superconductivity emerges. The $T_c(x)$ dependence in HTSC shows that superconductivity begins above a certain critical concentration x_1 , where x is the concentration of charge carriers n_f . For n_f above x_1 , T_c increases until the optimal concentration x_{opt} reaches and decreases with a further increase in x (Fig. 2). For n_f below x_{opt} , there are two characteristic temperatures, namely the *pseudogap opening temperature* T^* and T_c . At $T_c < T < T^*$, a phase of incoherent pairs (so-called local pairs (LPs)) sets in, but only at $T=T_c$ does phase coherence arise and the system goes over into a superconducting state. The existence of

these two characteristic temperatures reflects various phenomena associated with strong electronic interactions.

As can be seen from Fig. 2, which shows the generalized phase diagram of HTSC in coordinates $T(x)$ (T is the temperature, x is the concentration of charge carriers, which are holes in cuprates of the YBCO type), there are at least four distinct regions in which the physical properties of HTSCs differ dramatically. At low concentrations x , the system is in the dielectric antiferromagnetic (AF) state, and the localization of spins and charge carriers is observed. The superconducting (SC) region, the so-called SC - dome, is located between two threshold concentrations: x_1 and x_{max} . Above the SC - dome, there are two more distinct areas, conventionally separated by the line $T^*(x)$. Above this line is the so-called normal state area. According to the theoretical NAFL model [51], this region is characterized by a stable scattering intensity of normal carriers, which is a reliable sign of the normal state of the system. Below the $T^*(x)$ line there is a region of the PG state. At-present, literary sources actively discuss two main scenarios for the appearance of a PG anomaly in HTSC systems. According to the first, the occurrence of PG is associated with fluctuations of short-range order of the "dielectric" type, for example, antiferromagnetic fluctuations, waves of spin and charge density, etc. (see, for example, [11,12] and the survey [52]). The second scenario assumes the formation of paired fermions (most likely in the form of LPs [3]) already at temperatures much higher than the critical temperature $T^* \gg T_c$ with the subsequent establishment of their phase coherence at $T \leq T_c$ [3,50,52]. Intensive discussions on this issue continue to this day [3-7,10,11]. The question also remains whether T^* tends to zero along with T_c , as shown in Fig. 2, or it cuts the SC dome at approximately x_{opt} level and crosses the x -axis at the so-called quantum critical point [10,11].

2.2. The effect of pressure on the phase state of HTSC compounds of the 1-2-3 system.

One of the first and most detailed experimental studies of the effect of pressure on T_c in the $YBa_2Cu_3O_{7-\delta}$ HTSC system (1-2-3 system) was undertaken by Griessen's group [54]. In this case, it followed from the generalized data that the baric derivative dT_c/dP is positive and substantially depends on the charge carrier concentration n . It reaches a maximum in samples with a reduced $T_c \approx 25$ K and tends to a minimum when T_c reaches the highest values $T_c \approx 90$ K.

A set of studies of various physical properties of high-temperature superconducting compounds of the 1-2-3 system based on yttrium show the presence of a nonequilibrium state in such structures with a certain degree of oxygen deficiency. In this case, external factors, such as temperature and high pressure [55-57], play a significant role leading to a change in the lattice parameters and inducing processes of redistribution of labile oxygen,

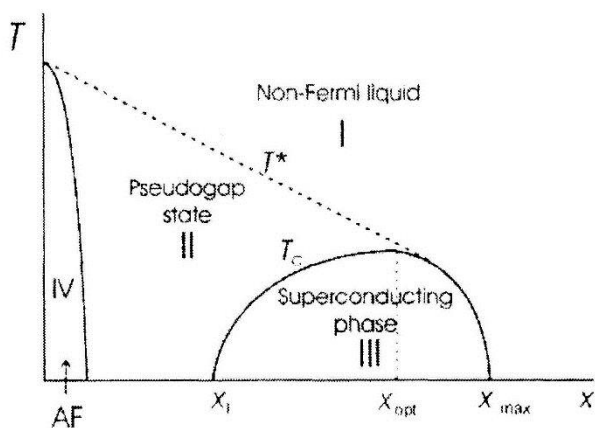


Fig. 2. HTSC phase diagram.

which, in turn, affects the critical parameters of the superconductor.

According to [58], the dependence of the critical temperature (T_c) on the pressure $T_c(P)$ for the YBCO system can be represented as:

$$T_c(P) = T_c + \frac{T_c}{T_c^{\max}} \Delta T_c^{\max}(P) + T_c^{\max}(P) \beta [2(n^{\text{opt}} - n) - \Delta n(P)] \Delta n(P) \quad (5)$$

where T_c^{\max} is the maximum value of T_c in this compound, $n^{\text{opt}} = (n^{\text{min}} + n^{\text{max}})/2$, $\beta = 1/(n^{\text{min}} + n^{\text{max}})^2$. For YBCO, n^{min} is the minimum number of holes per CuO_2 plane, at which superconductivity appears, equal to 0.06 holes per plane, n^{max} is the maximal number of holes per CuO_2 plane, at which superconductivity disappears and n^{opt} is the number of holes per CuO_2 plane, at which $T_c = T_c^{\max}$, equal to approximately 0.25 holes per CuO_2 plane [58].

In this expression, the second term characterizes the change in T_c under pressure associated with a change in the lattice parameters, electron-phonon interaction, bonds between layers, etc. - the so-called "true" pressure effect. The third term is due to a change in the number of holes under pressure - the so-called "relaxation" effect associated with the redistribution of labile oxygen. Summarizing the theoretical and experimental data available to date, we can conclude that it is essential to separate the "true" and "relaxation" pressure effects. In this section, we will try to briefly discuss each of these mechanisms.

2.3. The "true" pressure effect. One of the possible explanations for the peculiarities of the $T_c(P)$ dependences in the 1-2-3 system was proposed in the theoretical Saiko-Gusakov model [59], which relates the change in the temperature of the superconducting transition with the peculiarities of the dynamics of the apical O(4) atoms, which form a bistable sublattice controlled by the application of external pressure and a change in oxygen nonstoichiometry. According to [59], the birth of a 90-degree phase when pressure is applied to a sample of a 60-degree phase or the alternation of the same phases with varying oxygen nonstoichiometry is due to the "switching" of the frequency of the mode dominating in BCS pairing due to the transformation of the bistable potential of apical oxygen atoms. At the same time, as x decreases, the amount of pressure required to transfer the system to the 90-degree phase also decreases. Thus, a significant increase in T_c upon application of pressure is interpreted as an extended transition from the 60-degree phase to the 90-degree phase. Indeed, as can be seen from Fig. 3, which

shows the diagram $T_c \sim \frac{d \ln T_c}{d \ln V(T_c)}$ of crystals K2, K4, and

K7, calculated with taking into account the bulk moduli (100 GPa at $x < 0.1$ and 115 GPa at $x > 0.1$ [60]), there is a

break in the dependencies $\frac{d \ln T_c}{d \ln V(T_c)}$, which may indicate

a transition from a 60-degree phase to a 90-degree phase, differing in dT_c/dP .

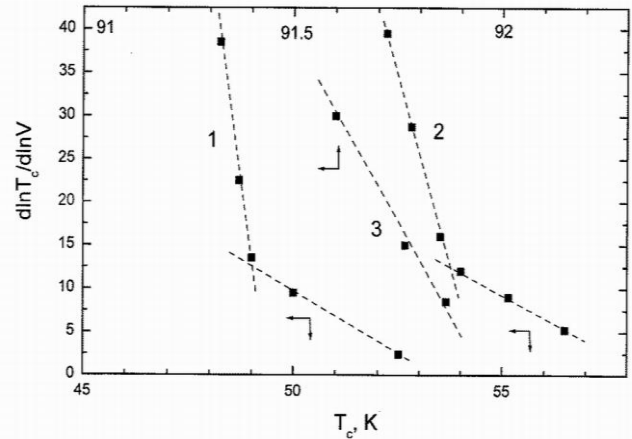


Fig. 3. Diagram $T_c \sim d \ln T_c / d \ln V$ of $\text{YBa}_2\text{Cu}_3\text{O}_{7-\delta}$ crystals with oxygen deficiency $\delta \approx 0.5$ and $\delta \approx 0.45$ (1, 2), as well as a sample of composition close to stoichiometric $\delta \approx 0.1$ (3), calculated with taking into account the bulk moduli (100 GPa at $x < 0.1$ and 115 GPa at $x > 0.1$ [60])

However, the anomalous increase in dT_c / dP obtained in this work from 1.5 to 2.5 K kbar⁻¹ in the region of low pressures up to 1.2 kbar with an insignificant difference in the oxygen content in samples with T_c 45 and 50 K, as well as a change in the sign of dT_c/dP at uniaxial pressure in different crystallographic directions [61], apparently, does not allow to unambiguously explain the features of the $T_c(P, x)$ dependences only within the framework of the indicated theoretical model.

Possibly, the features of the behavior of the $T_c(P, x)$ dependences are a consequence of several mechanisms, one of which is associated with a change in the band structure under the action of uniform compression. The observed linear relationship $\frac{d \ln T_c}{d \ln V(T_c)}$ and $d \ln T_c$ can be

obtained within the framework of the theoretical Labbe - Bock model [62], which takes into account the contribution of the logarithmic singularity to the density of states of the half-filled band. In this model, T_c is given by:

$$T_c = D \cdot \exp\left(\frac{-1}{\lambda^{1/2}}\right) \quad (6)$$

where D is the "width" of the singularity. Then for the volume dependence of T_c we have

$$\frac{d \ln T_c}{d \ln V} = \frac{d \ln D}{d \ln V} + \frac{1}{2\lambda^{1/3}} \frac{d \ln \lambda}{d \ln V}$$

This implies

$$\frac{d \ln T_c}{d \ln V} = a_1 \ln T_c + a_2, \quad (7)$$

$$a_1 = -\frac{1}{2} \frac{d \ln \lambda}{d \ln V}; \quad a_2 = \frac{d \ln D}{d \ln V} - a_2 \ln D$$

The kinks in the dependences $\frac{d \ln T_c}{d \ln V(T_c)}$ can be

associated with the cluster structure of the sample, which is confirmed by the presence of steps on the resistive transitions to the superconducting state. As shown in [23], the observed stepwise form of resistive transitions indicates a nonstoichiometric ratio of the concentrations of oxygen and vacancies, which leads to the formation of a mixture of phase clusters that are characterized by different oxygen contents and ordering, and, accordingly, have different critical temperatures and values dT_c/dP .

The relatively weak effect of pressure on the T_c value of optimally doped samples can be explained within the framework of a model assuming the presence of a Van Hove singularity in the spectrum of charge carriers [62,63] which is characteristic of strongly coupled lattices. As is known, for crystals with $T_c \approx 90\text{K}$ the Fermi level lies in the valley between two peaks of the density of states, while the density of states at the Fermi level $N(E_F)$ depends significantly on the difference $(a-b)/a$ [62,63]. An increase in the $(a-b)/a$ ratio leads to an increase in the distance between the peaks of the density of states and, accordingly, to a decrease in $N(E_F)$ and T_c . Accordingly, a decrease in the $(a-b)/a$ ratio leads to a convergence of the peaks of the density of states, which leads to an increase in $N(E_F)$ and T_c . Such a regularity of the change in T_c was observed when studying the effect of uniaxial compression along the a and b axes on the critical temperature of single crystals with $T_c \approx 90\text{K}$ [61]: when a load was applied along the a axis, the critical temperature increased, and when a load was applied along the b axis, it decreased. Under the influence of hydrostatic pressure, the value of the ratio $(a-b)/a$ changes insignificantly, since it is determined only by the difference in the compression moduli along the a and b axes. Therefore, the change in the critical temperature when exposed to hydrostatic pressure is relatively small.

For crystals with $T_c \approx 60\text{K}$, the Fermi level is shifted from the middle of the band and is located away from the

Van Hove singularity. Therefore, if the value of the critical temperature is primarily determined by the density of electronic states, then under the action of hydrostatic pressure the Fermi level should shift towards the peak of the density of states.

It is interesting to note that we observed similar features of the behaviour of the baric derivatives dT_c/dP depending on the change in composition in NbSe_2 single crystals, which also belong to systems of two-dimensional lattices and have a similar anisotropy parameter [64-66]. Thus, for example, intercalation with deuterium up to 2 at.%, as well as the introduction of tin impurities into the composition of niobium diselenide leads to an increase in dT_c/dP by a factor of 2-3 in comparison with the pure sample. In this case, an increase in dT_c/dP is observed with an increase in the concentration of tin impurities. It should also be noted that the behaviour of the pressure dependences $T_c(P)$ is qualitatively the same for single-crystal NbSe_2 and YBCO. These features in the $T_c(P)$ dependences were interpreted as a consequence of a shift of the Fermi level relative to the root features of the density of states.

2.4. Phase separation and relaxation effect of pressure. An important feature was first established by Driessen et al. [67]: the baric derivatives dT_c/dP of the beginning and end of the phase transition to the SC state of the YBCO compound have opposite signs in the pressure range from 0 to 170 Kbar. In this case, the negative derivative $dT_{cf}/dP < 0$ corresponds to the low-temperature phase, and the positive derivative $dT_{co}/dP > 0$ corresponds to the high-temperature phase. Thus, the application of high pressure leads to the expansion of the temperature range $(T_{co}..T_{cf})$ corresponding to the realization of the fluctuation paraconductivity regime at $T > T_c$.

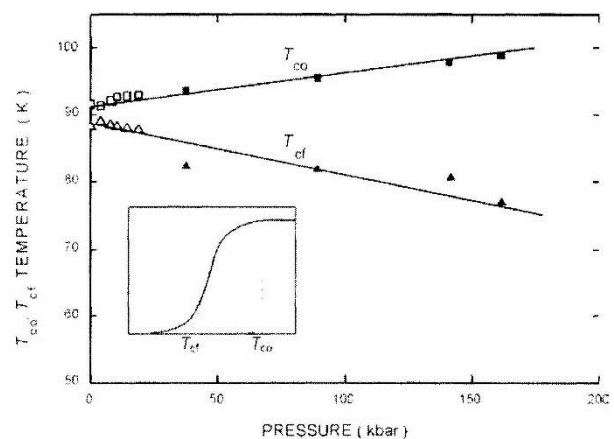


Fig. 4. Pressure dependence of T_{co} и T_{cf} for YBCO [68]. Inset: T_{co} is the critical temperature of the beginning, and T_{cf} is the temperature of the end of the superconducting transition.

As is known from the literature [69-71], in HTSC cuprates, the $T_c(x)$ dependence is fairly well described by the universal parabolic dependence:

$$T_c = T_c^{\max} [1 - A(x - x_{\text{opt}})^2], \quad (8)$$

where T_c^{\max} , A , x и x_{opt} are functions of pressure. As mentioned above, in YBCO, the charge carrier concentration can be changed by changing the oxygen concentration by cationic substitution or by applying pressure.

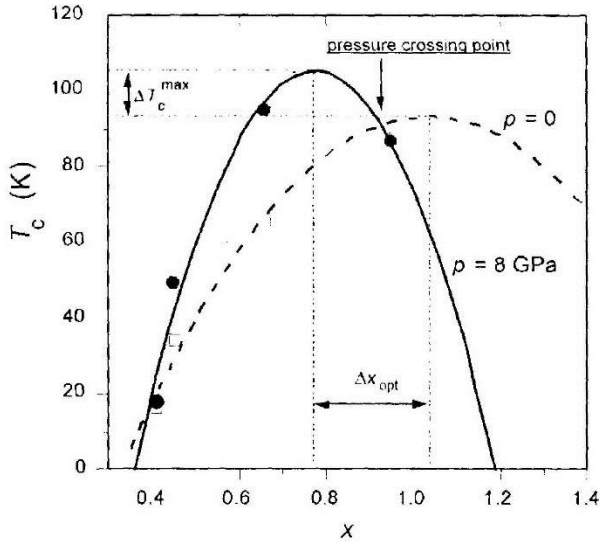


Fig. 5. T_c as a function of the oxygen content x for $\text{YBa}_2\text{Cu}_3\text{O}_{6+x}$ at pressures $p = 0$ to $p = 8$ GPa. The constructed parabolic approximation of the experimental data at $p = 8$ GPa is taken from Ref. [71].

This dependence correctly describes $T_c(x)$ for compounds such as $\text{YBa}_2\text{Cu}_3\text{O}_{6+x}$, $\text{Y}_{1-x}\text{Ca}_x\text{Ba}_2\text{Cu}_3\text{O}_6$, $\text{La}_{2-x}\text{Sr}_x\text{CuO}_4$, $\text{La}_{2-x}\text{Sr}_x\text{CaCu}_2\text{O}_6$, as well as for $(\text{Ca}_x\text{La}_{1-x})(\text{Ba}_{1.75-x}\text{La}_{0.25+x})\text{Cu}_3\text{O}_y$ for different oxygen concentration y .

The critical temperature depends not only on the concentration of charge carriers, but also on the binding strength in the CuO_2 planes, on the propagation of structural phase transformations, and on the pressure caused by relaxation phenomena. An interesting effect has been discovered associated with the degree of ordering of the defects of labile oxygen in the lattice: an increase in pressure decreases the mobility of defects and at the same time increases the degree of ordering of oxygen defects. This effect is very well observed in YBCO samples with a reduced oxygen content [71], in which T_c increases with pressure and, therefore, the dT_c/dp value strongly depends on the temperature at which the pressure applied.

It should also be added that in his studies of fluctuation effects [72], Abrikosov suggested the formation of superconducting strings, the so-called “stripes,” in one preferred crystal direction, in other words, one-dimensional superconducting channels. Such channels appear far from the percolation threshold and can increase the superconductivity of the sample. An inhomogeneous

contribution of carriers and strong fluctuations are inherent in superconductors with a low carrier concentration, for which there are two characteristic temperatures T^* and T_c , as well as charge and spin pseudogaps.

As mentioned above, for a low carrier concentration ($x_1 < x < x_{\text{opt}}$) at T^* , fermions begin to combine into local pairs (complex bosons), which condense at $T_c \ll T^*$. For high carrier concentrations ($x_{\text{opt}} < x < x_{\text{max}}$), both characteristic lines eventually merge and $T^* = T_c$ (refer to Fig. 2), which means that the formation of Cooper pairs occurs at the same temperature as superconducting condensate. The pair correlation line can be considered as the line of boson production, reaching macroscopic phase coherence only at the temperature T_c , below which the entire system is described by a single wave function.

In the Miknos-Robazhkevich model of local pairing [73], the pressure effects measured by dT_c/dp are determined differently on both sides of the optimal carrier concentration. The transfer integral increases with increasing pressure. Therefore, the pressure coefficient is positive below x_{opt} and T_c is measured as $t^2/|U|$. Since at x above x_{opt} T_c is measured as $1/2zt$, the pressure coefficient is negative (as in the BCS model) (Fig. 6).

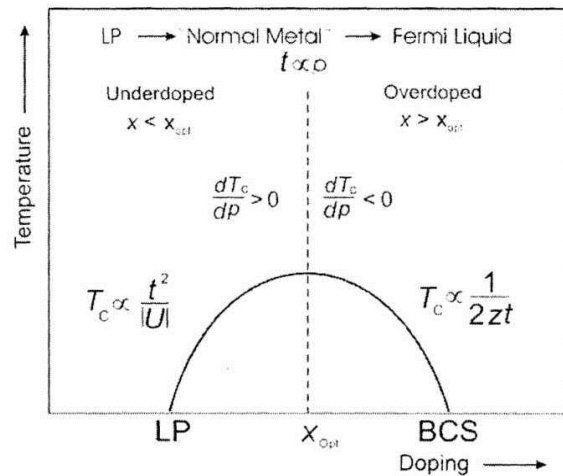


Fig. 6. Scaling the pressure effect below ($x < x_{\text{opt}}$) and above ($x > x_{\text{opt}}$) the optimal carrier concentration [73].

Near T_c^{\max} , the pressure coefficient is approximately 0. Therefore, the pressure causes an increase in T_c in the concentration regime, where there are two special characteristic temperatures T^* and T_c . If $T^* = T_c$, then the pressure coefficient is negative and T_c decreases by pressure, as in "classical" superconductors. This dependence was confirmed experimentally in the case of the YBCO compound [74], for which a positive and negative pressure coefficient of T_c was observed.

Recent calculations by Miknas and Tobiyazhevsky show that the broadening of the pseudogap region associated with the overlap of the S- and D- wave components causes an additional increase in T_c in the low doped regime [75]. Above the concentration x_{opt} , the $T^*(x)$ lines merge with the $T_c(x)$ line, and Bose-Einstein condensation (BEC) takes place in the metallic region, where charge and phase fluctuations can be neglected, as in the BCS model [3]. Therefore, the pressure effect is negative here. However, the shift in x_{max} for lower concentrations is still experimentally unconfirmed.

2.5. High-pressure-induced diffusion of the labile component in the $Y_1Ba_2Cu_3O_{7-\delta}$ compound. In the case of HTSCs, diffusing oxygen defects are usually already present due to the synthesis procedure. Assuming that the total defective volume is zero, we can write:

$$\Delta V_A \approx \Delta V_M \approx N_A \frac{\partial E_A}{\partial P}$$

This expression for the migration volume has a simple physical interpretation. If an ion diffuses from one cell to another, it must overcome the energy barrier E_A caused by its interaction with the ionic environment. In the presence of pressure P , the free movement of ions inside the crystal becomes extremely difficult, since they must now do work against the external pressure $\Delta E_A = P\Delta V_M$, which increases the activation energy by ΔE_A . In the hard-sphere model, each ion interacts with its neighbors like a rigid ball with its own ionic radius corresponding to its valence. The migration volume V_M can be estimated by calculating local expansions, which look like migrating solid ionic spheres "pushing" each other towards the so-called "saddle point" [71]. Since the calculated value ΔV_M depends on the sum of the individual diffusion contributions, the measurement $\frac{\partial E_A}{\partial P}$ can be used to study diffusion processes in compounds 1-2-3.

At present, the ionic radii of the ions of interest to us have been calculated: $r(Cu^{1+}) = 0.96 \text{ \AA}$, $r(Cu^{2+}) = 0.72 \text{ \AA}$, $r(O^{2-}) = 1.32 \text{ \AA}$, $r(Ba^{2+}) = 1.34 \text{ \AA}$. All ions are assumed to be solid balls. The change in volume due to the diffusion movement of ions through the "saddle point" is considered local. We will assume that only the nearest neighbors that are in direct contact with the ion under consideration can contribute to the change in the migration volume. In our calculations, we assume that this motion affects the volume, which extends up to half the distance to the nearest neighbors in the direction perpendicular to the motion of this ion since it is assumed that these neighbors remain at their lattice sites, independent of the diffusion process. Using these general procedures, we can now calculate the

corresponding volumes. Let us consider this effect by the example of $Y_1Ba_2Cu_3O_{7-\delta}$.

The Y-123 system has an orthorhombic structure shown in Fig. 7 (a). Oxygen ions O^{2+} occupy the O(1) states between $Cu^{1+/2+}$ along the b axis. The O(5) states between Cu ions along the a axis are unoccupied. While the O(1) states are only partially occupied, oxygen vacancies are already present in the structure, which confirms the previous assumptions and $\Delta V_F = 0$. For the calculation ΔV_M , all local diffusion paths should be summed up. There is still no agreement in the literature on the dominant oxygen diffusion pathway in Y-123: different authors propose different paths. However, most authors assume that oxygen diffuses through the center of the cell in the Cu-O layer of the chain.

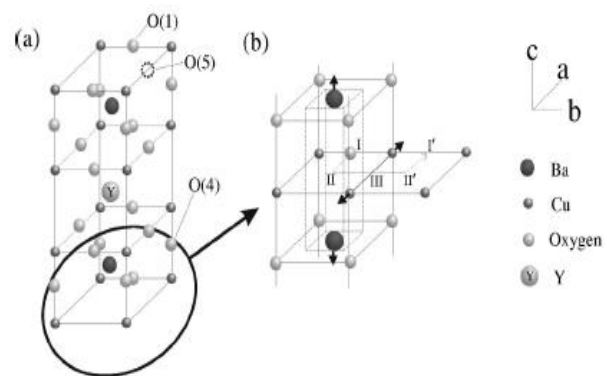


Fig. 7. Calculation of the migration volume in Y-123. a) Orthorhombic structure Y-123. b) Corresponding part of the Y-123 structure with a Ba-O layer and a Cu-O layer. The diffusion path is indicated by the dashed line, and the dashed box represents the volume used in the assessment [71].

We will assume that (Fig. 7 (b)) the vacancy passes from the O(1) (I) state in the center of the cell (II) to the adjacent O(5) (III) states, and then through the center of the next cell (II') returns to empty state O(1) (I'). There are two different transition configurations for this process: (i) when O^{2-} is located in the center of the cell between two Ba^{2+} ions (II) and, (ii) when O^{2-} occupies the O(5) position in the lattice site (III).

In the first case, we assume that no changes occur in the ab plane. Thus, the general increase in volume is associated with Ba^{2+} ions moving along the c axis in the other direction relative to the direction of diffusion of oxygen ions. The hatched parallelepiped indicates the volume of interest to us in Fig. 7 (b). For $Y_1Ba_2Cu_3O_{6.41}$, the area of the base of this parallelepiped in the ab -plane is 3.73 \AA^2 . The open space between Ba^{2+} ions in the initial configuration is $2z(Ba^{2+}) - 2r(Ba^{2+}) = 1.80 \text{ \AA}$, where $z(Ba^{2+})$ means the atomic position of the Ba^{2+} ion. Since the diameter of the O^{2-} ion is 2.64 \AA , the Ba^{2+} ions must move outward by 0.84 \AA (0.42 \AA for each Ba^{2+} ion) to satisfy the conditions for the transition to the configuration

of the O^{2-} (II) ions. In this case, the volume of the shaded parallelepiped in Fig. 7 (b) should change by $\Delta V_M \approx +3.13 \text{ \AA}^3$, changing the migration volume by $\Delta V_M \approx +1.88 \text{ cm}^3 / \text{mol}$. Similar calculations for $Y_1Ba_2Cu_3O_{6.45}$ with a higher oxygen concentration yield $V_M \approx +1.9 \text{ cm}^3 / \text{mol}$, since the Ba^{2+} ions are slightly closer to each other. For $Y_1Ba_2Cu_3O_{6.6}$, the migration volume is calculated as $V_M \approx +2.05 \text{ cm}^3 / \text{mol}$.

To calculate the second case (II) with O^{2-} between two Cu ions in the ab -plane, it is assumed that no changes along the c axis occur [Fig. 7 (b) position III]. The open space between two Cu ions is 2.17 \AA (it is assumed that one of them is a Cu^{2+} ion, the other is a Cu^{1+} ion). Thus, two Cu ions need to move by 0.47 \AA to accommodate O^{2-} ions, changing the migration volume by $V_M \approx +1.24 \text{ cm}^3 / \text{mol}$. Slightly lower than case (i). An experimentally determined activation volume can provide information on the increase with pressure in the maximum activation energy along the diffusion path. The fact that the O(5) state is almost equivalent to the O(1) state shows that the barrier for the transition point is lower than for position II, where the oxygen ion is sandwiched between two Ba^{2+} ions. Thus, we can assume that the inflection point at position II determines the migration volume for this diffusion path. Calculations of the migration volume give the value $V_M \approx +1.9 \text{ cm}^3 / \text{mol}$ for $Y_1Ba_2Cu_3O_{6.4}$ and for $Y_1Ba_2Cu_3O_{6.45}$, which is approximately half the calculated value in previous works. The analysis of the experimental data allows us to conclude that none of the two diffusion pathways described above is excluded.

2.6. The influence of a magnetic field on excess paraconductivity. As shown in [76], the general expression for the fluctuation paraconductivity $\Delta\sigma(T, H)$ of layered superconductors in a magnetic field can be written in the form:

$$\Delta\sigma(T, H) = \Delta\sigma_{AL}(T, H) + \Delta\sigma_{MT}(T, H)$$

where

$$\Delta\sigma_{AL}(T, H) = \frac{e^2}{16hd\varepsilon} \times \left\{ \frac{1}{(1+2\alpha)^{1/2}} - \frac{(2+4\alpha+3\alpha^2)b^2}{4(1+2\alpha)^{5/2}\varepsilon^2} + \dots \right\} \quad (10)$$

is Aslamazov-Larkin fluctuation conductivity [45];

$$\Delta\sigma_{MT}(T, H) = \frac{e^2}{8hd(1-\alpha/\delta)\varepsilon} \times \left\{ \ln\left(\frac{\delta}{\alpha} \frac{1+\alpha+\sqrt{1+2\alpha}}{1+\delta+\sqrt{1+2\delta}}\right) - \left[\frac{\delta^2}{\alpha^2} \frac{1+\delta}{(1+2\delta)^{3/2}} - \frac{1+\alpha}{(1+2\alpha)^{3/2}} \right] \frac{b^2}{6\varepsilon} + \dots \right\}$$

is the Maki-Thompson fluctuation conductivity [77] due to the interaction of unpaired charge carriers with fluctuation Cooper pairs; d is the thickness of the two-dimensional layer; $\alpha = 2\xi_c^2(0) / d^2\varepsilon$; $b = (2e\xi_{ab}^2(0) / \hbar H$; $\delta = (16/\pi)(\xi_c^2(0) / d^2)(kT\tau_\phi / \hbar)$; $\xi_{ab}(0)$ is the coherence length in the basal plane and τ_ϕ is a phase relaxation time of the fluctuating pairs. For example, the effect of a magnetic field on the pseudogap temperature was studied in [53].

3. Crystal structure of dichalcogenides.

Transition metal chalcogenides form a broad class of layered compounds, the physical properties of which depend on the structure, composition, type of transition element, chalcogen, and stoichiometry [64,78]. Dichalcogenides of transition metals have a layered structure and are designated by the Formula NK-MX, where N is the number of layers per unit cell, K is the type of unit cell (H is hexagonal, R is rhombohedral), M is a transition metal of 4-6 groups, for example, Nb, Ta, W and X - chalcogen (S, Se, Te). The crystals of these compounds are composed of layers, each of which is a sandwich of two layers of halogen atoms X with a layer of metal M atoms between them. The bond between the metal and halogen atoms in the sandwich is strong (predominantly covalent), and the M and X atoms in the sandwich form a two-dimensional hexagonal lattice. The MX layers are interconnected in the crystal by weak Van der Waals forces [78]. The schematic structure of the crystal is shown in Fig. 8.

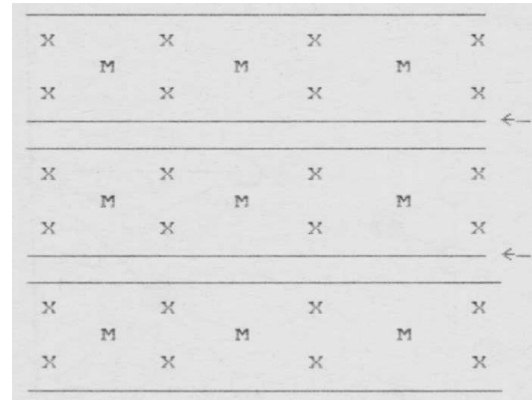


Fig. 8. Layer structure of transition metal dichalcogenides. View in a direction parallel to the layers. The arrows point to the Van der Waals links [78].

There are two ways of arranging chalcogen atoms around a metal atom, in the first case forming an octahedron, and in the other, the same number of atoms- a trigonal prism while maintaining the hexagonal packing of the layer. In $2H-NbSe_2$, the environment of the metal ion forms a trigonal prism (rhombohedral) (Fig. 9).

The structure of 2H-NbSe₂ makes it easy to introduce various atoms or molecules into the Van der Waals gap, thus increasing the distance between the layers of the "sandwich", and also changing the concentration of free electrons in the layers due to the donor or acceptor properties of the intercalant or impurity, which makes it possible to study the effect of changes in the electronic and phonon spectrum on the superconductivity of layered crystals.

The anisotropy of the crystal structure determines the anisotropy of the kinetic and thermodynamic properties of these compounds. Electrical conductivity, compressibility, coefficient of thermal expansion can differ by several orders of magnitude along and across the layers. When studying the microcontact spectra of the electron-phonon interaction (EPI) in 2H-NbSe₂, the anisotropy of the EPI spectra was found for contacts oriented along the *c* axis and parallel to the basal plane. In this case, a shift of the high-frequency edge of the spectrum from the energy range of about 40 meV was observed for contacts whose axis was oriented parallel to the *c* axis of the 2H-NbSe₂ crystal to the energy range near 60 meV for contacts oriented parallel to the basal plane [79].

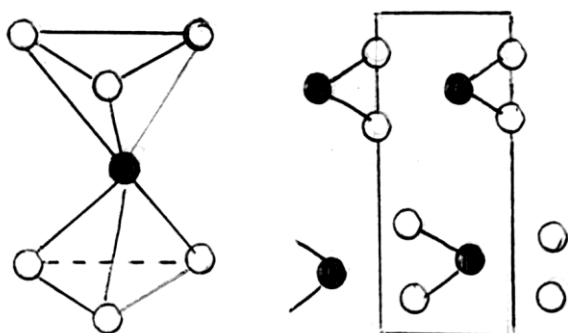


Fig. 9. The mutual arrangement of atoms in the coordination cell inside the sandwich [78].

More detailed information on the structure and physical properties of TMDs can be found in [78].

3.2. Band structure and Fermi surface. Studies of the topology of the Fermi surface of transition metal dichalcogenides by traditional methods, for example, magnetoacoustic, used for pure metals, are unsuitable due to the small value of the free path of charge carriers (10^{-8} m). Therefore, there is a small amount of experimental work where magnetoresistance, magnetic susceptibility (oscillatory part), and magnetothermal oscillations have been studied. Most of the experimental methods used to study the Fermi surface require a theoretical model to interpret the results obtained. In particular, to determine whether specific oscillations belong to the electron or hole Fermi surface. In this regard, theoretical models are

essential, which provide at least a qualitative description of the band structure and the Fermi surface, as well as indirect experimental data characterizing the Fermi surface, the electronic energy spectrum, methods of varying the electron density due to the intercalation process, measuring the effect of uniaxial and hydrostatic pressures to change the kinetic and thermodynamic properties of 2H-NbSe₂.

The general topological features of the Fermi surface were obtained in the calculations of Mattheis [80]. As indicated in [81], the Fermi surface for 2H-NbSe₂ consists of hole pockets grouped along six NK axes and a hole surface at the center of the band, which is a corrugated cylinder elongated along the *c* axis. Also, it is extremely important that, as shown in Ref. [82], the Fermi level can lie near singular points, such as saddle points, which are characterized by a low Fermi velocity. Small electron pockets in the center of the band experimentally discovered in Ref. [83] can be obtained in theoretical models with allowance for the interlayer interaction; however, there are still many ambiguities. That is why indirect experimental data characterizing the Fermi surface and the electronic energy spectrum are essential.

3.3. Structural phase transitions of the CDW type in systems with a reduced dimension. Solids that have a regular crystal lattice with a clearly expressed translational symmetry, under certain conditions, can become unstable concerning small distortions in the arrangement of atoms. Then such a stable state can arise in which the charge density or the position of atoms have long-period modulations. The modulation period can be comparable or incommensurate with the period of the main lattice. Transitions of this kind are called charge density wave (CDW) transitions and are classified as commensurate CDW (CCDW) and, accordingly, incommensurate CDW (UCDW). CDW transitions were found in many-layered and quasi-one-dimensional structures, such as intercalated graphite compounds, layered dichalcogenide conductors, NaNO₃, K₂SO₄, and NbSe₂ dielectrics [84,85]. In NbSe₂, a CDW-type structural transition was found at $T=33$ K. These transitions are apparently first-order transitions. They are manifested primarily in changes in the kinetic and magnetic properties of these compounds. According to modern concepts [1], the appearance of these structural transitions is associated with the presence on the Fermi surface of regions that can be aligned with each other when shifted in momentum space by a certain vector. If the sections are displaced relative to each other by the vector *q*, then below T_{CDW} there appears a sinusoidal displacement of atoms from the position of equilibrium with the wave vector *q*. In the case of a two-dimensional or three-dimensional lattice, when the Fermi surface also contains mismatched regions, the transition with the appearance of a superstructure - a charge density wave - turns out to be a

metal-metal or metal - semimetal transition, depending on the area of the overlapping sections of the Fermi surface. In 2H - modifications of MX_2 , an incommensurate CDW arises, which can be described by three vectors

$$\vec{q} = \frac{1}{3} \vec{b}^* (1 - \delta),$$

where b is the inverse vector of the original lattice, δ is the incommensurability parameter. For 2H-NbSe₂ $\delta \approx 0,02$. The coexistence of superconductivity and CDW was found in 2H-TaS₂, 2H-NbSe₂. However, since both of these phenomena compete with each other due to pieces of the Fermi surface with a high density of states at the Fermi level, $N(E_f)$, the onset of CDW manifests itself in the suppression of superconductivity. For example, when the compound 2H-TaS₂ is intercalated with various organic molecules, CDW is suppressed by decreasing the wave amplitude, or the temperature of its occurrence, T_{CDW} , and, at the same time, an increase in T_c is observed. Suppression of CDW can be realized by applying external pressure to the sample or by introducing impurity atoms.

3.4. Influence of intercalation and high pressure on the conductivity of the layered dichalcogenide conductors. The presence of a weak Van der Waals bond between the layers in MX compounds suggests that their critical temperature is strongly dependent on the interaction of the layers, and, with an increase in this interaction, T_c should increase due to the suppression of two-dimensional fluctuations. This conclusion is based on the fact that, in the $\text{Nb}_{1+x}\text{Se}_2$ compound, the distance between the layers increases with increasing x , and T_c decreases [86].

Back in 1976, Jerome and others [87, 88] found that when hydrostatic pressure was applied to 2H-NbSe₂, T_{CDW} decreased with increasing pressure, while T_c increased. This continued up to $P \approx 36$ kbar, at this pressure $T_{\text{CDW}} = T_c$ and no further increase in T_c was observed, up to 140 kbar. It was concluded that there is an unambiguous relationship between the dependences $T_c(P)$ and $T_{\text{CDW}}(P)$. Hydrostatic pressure suppresses the CDW transition, which leads to an increase in T_c up to pressures corresponding to $T_c = T_{\text{CDW}}$.

The authors of [89] first studied the effect of hydrogen intercalation on $R(T)$ of 2H-NbSe₂ single crystals. Depending on the degree of intercalation, T_{CDW} of the initial crystal decreases from $T_{\text{CDW}} = 33$ K to $T_{\text{CDW}} = 12$ K, and simultaneously T_c decreases from 7.2 K to $T_c < 4.2$ K. With a significant nonlinear decrease in T_{CDW} and a shift of T_c toward lower temperatures, the width of the resistive transition changes insignificantly. Hydrogen is a donor. It donates its electron to the layer of the intercalated crystal. The authors of [90] first performed the intercalation of NbSe₂ with an acceptor. This intercalant is the TCNQ

molecule, an organic molecule with a strong acceptor property. It was shown that, depending on the degree of intercalation, an increase in T_{CDW} was observed up to 40-50 K, while T_c decreased and stabilized in the region of 5-6 K.

However, these studies were carried out without applying pressure. Sambongi [91] performed uniaxial compression along the c axis in 2H-NbSe₂. It was found that T_c decreases in this case, reaching saturation at approximately the same pressures as under hydrostatic conditions. All these facts served as the basis for the conclusion about the negligible effect of interlayer interaction on T_c . But Sambongi began research in the area of 5 kbar. Thus, the region of low pressures was out of the field of view of the experimenters.

This gap was corrected by the authors of [92]. They investigated the effect of uniaxial pressure on T_c of compounds NbSe₂ and Nb_{0.9}Sn_{0.1}Se₂. In this work, it was found that with an increase in pressure from 0 to 3 kbar, T_c increases from 7 K to about 7.6 K, and with a further increase in pressure from 3 to 6 kbar, T_c decreased from 7.6 to 6.8 K. Authors have proposed the model in which it was shown that the peak in the $T_c(P)$ dependence is associated not with the degradation of the CDW transition, but with a change in the band structure under the influence of pressure.

Thus, the growth of T_c under pressure is not unambiguously explained only by the suppression of the charge density wave. One should take into account the change in the carrier density at the Fermi level $N(E_f)$, which is not associated with the suppression of CDW, and, in addition, the change in the electron-phonon interaction constant (I). Indeed, as shown in ref. [93], the increase in $N(E_f)$ due to suppression of CDW cannot exceed 10% by the NMR method. For compounds intercalated by deuterium, the application of a pressure of 12 kbar leads to an increase in T_c by 20%, while T_{CDW} decreases by only 8%. The application of hydrostatic pressure up to $P = 13$ kbar leads to a linear decrease in T_{CDW} at a rate of $dT_{\text{CDW}} / dP = -0.16$ K / kbar and to a simultaneous increase in T_c , with $dT_c / dP = 0.12$ K / kbar at $0 < P < 7$ kbar and 0.07 K / kbar in the region $7 < P < 13$ kbar. Thus, $dT_c / dT_{\text{CDW}} = -0.75$ and -0.45 in the indicated pressure ranges, which is 5 and 3 times higher, respectively, the rate of change of T_c when CDW is suppressed in pure 2H-NbSe₂.

Most of the work was carried out in the area of increasing anisotropy due to the iteration of the initial layered dichalcogenide conductors. It is of interest to study the decrease in anisotropy (which occurs as a result of the introduction of an impurity) due to the practically unaffected approach of the layers. On the other hand, the introduction of an impurity into the layered dichalcogenide conductors' lattice makes it possible to suppress the CDW,

change the phonon spectrum, the filling of the conduction band, and thus the density of electronic states at the Fermi level. The introduction of a tin impurity into the NbSe lattice is of particular interest from the point of view that makes it possible to consider the metal-semiconductor transition in the $\text{Nb}_{1-x}\text{Sn}_x\text{Se}_2$ system. Since NbSe₂ is a metal - a superconductor, and SnSe is a semiconductor with a layered hexagonal structure. Besides, the atomic radii of Sn and Nb are very close ($\text{Nb} = 1.45 \text{ \AA}$, $\text{Sn} = 1.46 \text{ \AA}$), and the introduction of tin should not lead to significant distortions of the lattice but can affect the filling of the conduction band, changes in the phonon spectrum and elastic properties.

In conclusion, it should be noted that this short literature review considers only a small part of the publications available in the literature devoted to various aspects of the electrical transport properties of layered compounds based on 1-2-3 HTSC systems and transition metal dichalcogenides under extreme external influences. Nevertheless, proceeding from the results of the analysis performed, a number of questions can be formulated that have not yet found a final experimental and theoretical solution. Namely, what is the role of the crystal lattice and structural defects and, in particular, twinning planes? How does the complete or partial replacement of the constituent components of HTSC compounds by their isoelectronic analogues affect the electroresistive characteristics? What is the reason for the broadening of the resistive transitions of HTSC compounds into the superconducting state under pressure, and what is the relationship between this broadening and charge transfer and the nature of the redistribution of the vacancy subsystem? What is the role of phase separation in the implementation of different modes of longitudinal and transverse transport?

Moreover, in this aspect, what is the mutual influence of PG- and SC-states? What is the role of similar physical characteristics and distinctive features between low-temperature and high-temperature superconductors associated with the crystal structure and the mechanism of superconductivity? Obviously, more research, both experimental and theoretical, is needed to answer these questions.

References/Literature

1. L. Li, J. Shen, Zh. Xu, H. Wang. International Journal of Modern Physics B, **19**, 275–279. (2005).
2. J.G. Bednorz, K.A. Muller. Phys. B, **64** (2), 189–193. (1986).
3. A.L. Solovjov Pseudogap and local pairs in high-Tc superconductors, *Superconductors – Materials, Properties and Applications* Ed. A. M. Gabovich, Chap. 7. (InTech., Rijeka, 2012), P.137–170.
4. D. Chakraborty, M. Grandadam, Hamidian M.H., J.C.S. Davis, Y. Sidis, C. Pépin. Phys. Rev. B, **100**. 224511 (1–33). (2019).
5. S.A. Kivelson S. Lederer. PNAS, **116**, 14395–14397. (2019).
6. N.J. Robinson, P.D. Johnson, T.M. Rice, A.M. Tselik. Rep. Prog. Phys., **82**, 126501. (2019).
7. V. Mishra, U. Chatterjee, J.C. Campuzano, M.R. Norman. Nat. Phys., **10**, 357–360. (2014).
8. T. Timusk and B. Statt Rep. Prog. Phys., **62**, 161–222. (1999).
9. R.V. Vovk, A.L. Solovjov. Low Temp. Phys., **44**, 111–153. (2018).
10. R.V. Vovk, M.A. Obolenskii, A.A. Zavgorodniy, A.V. Bondarenko, I.L. Goulatis, A.V. Samoilo, A.I. Chroneos. Journal of Alloys and Compounds, **453**, 69–74. (2008).
11. L. Taillefer. Annu. Rev. Condens. Matter Phys., **1**, 51–70. (2010).
12. S. Badoux, W. Tabis, F. Laliberté, G. Grissonnache, et al. Nature, **531**, 210–216. (2016).
13. R.V. Vovk, M.A. Obolenskii, A.V. Bondarenko, I.L. Goulatis, A.V. Samoilo, A.I. Chroneos, V.M. Pinto Simoes. J. Alloys and Compounds, **464**, 58– 66. (2008).
14. R.V. Vovk, M.A. Obolenskii, A.A. Zavgorodniy, A.V. Bondarenko, I.L. Goulatis, N.N. Chebotaev. Functional Materials, **14** (3), 302–308. (2007).
15. A.N. Bulaevsky UFN, (1975). **116** (3), 449–483. (A.N. Булаевский. УФН, **116** (3), 449–483. (1975)) [In Russian]
16. *Problema vysokotemperaturnoy sverkhprovodimosti* ed. V.L. Ginzburg, D.A. Kirzhitsa. (Nauka, Moscow, 1977), pp. 243–245 (*Проблема высокотемпературной сверхпроводимости*, ред. Гинзбург В.Л., Киржица Д.А. (Наука, Москва) с.243-245) [In Russian]
17. J.D. Jorgensen, P. Shiyou, P. Lightfoot, H. Shi, A.P. Paulikas, B.M.W. Veal. Physica C, **167** (3,4), 571–578. (1990).
18. R.J. Cava. Science. **247** (4943), 656–662. (1990).
19. M. Asta, D. de Futaie, G. Ceder, et.al. J. Less. Common Metals, **168** (1), 39–51. (1991).
20. T. Kemin, H. Meisheng, W. Yening. J. Phys. Condens. Matter., **1** (6), 1049–1054. (1989).
21. G. Lacayo, R. Hermann, G. Kaestener. Physica C, **192**, 207–214. 1992.
22. V.M. Pan, V.L. Svechnikov, V.F. Solovjov. Supercond. Sci. Technol., **5**, 707–711. (1992).
23. P.H. Kes Proceedings of the Los Alamos Symposium “Phenomenology and Application of HTSC”, 22–24. (1991).
24. W. Gawalek, W. Schueppel, R. Hergt. Supercond. Sci. Technol., **5**, 407–410. (1992).
25. V.V. Kvardakov, V.A. Somenkov, S.Sh. Shilstein. SFKHT, **5** (4), 624–630. (1992). (В.В. Квардаков, В.А. Соменков, С.Ш. Шильштейн. СФХТ, **5** (4), 624–630. (1992)) [In Russian]
26. V. Selvamanickam, M. Mironova, S. Son. Physica C. **208**, 238– 244. (1993).
27. G. Roth, G. Heger, P. Schweiss. Zh. Physica, **152** (4), 329–334. (1988).
28. G.D. Chryssikos, E.I. Kamitsos, J.A. Kapoutsis, et. al. Physica C, **254**, 44–62. (1995).
29. A.V. Bondarenko, A.A. Prodan, Yu.T. Petrusenko, et. al. Magnetic and superconducting materials, **A**, 499–506. (1999).
30. A.V. Bondarenko, A.A. Prodan, Yu.T. Petrusenko, et. al. Phys. Rev. B, **64** (9), 92513(1)–92513(4). (2001).

31. D.M. Ginzberg. Fizicheskiye svoystva vysokotemperaturnykh sverkhprovodnikov, (Mir, Moscow, 1991) 543 p. (Д.М. Гинзберг. *Физические свойства высокотемпературных сверхпроводников*, (Мир, Москва), 543 С.) [In Russian]
32. M.A. Obolenskiy, A.V. Bondarenko, R.V. Vovk, A.A. Prodan. FNT. **23** (11), 1178–1182. (1997). (М.А. Оболенский, А.В. Бондаренко, Р.В. Вовк, А.А. Продан. ФНТ. **23** (11), 1178–1182. (1997)) [In Russian]
33. M.A. Obolenskiy, A.V. Bondarenko, V.I. Beletsky, et al. Functional materials. **2** (4), 409–414. (1995). (М.А. Оболенский, А.В. Бондаренко, В.И. Белецкий, et al. Функциональные материалы. **2** (4), 409–414. (1995)). [In Russian]
34. R.V. Vovk, M.A. Obolenskii, A.A. Zavgorodniy, et al. J Mater Sci: Mater in Electron, **18**, 811–815. (2007).
35. M.A. Obolenskii, R.V. Vovk, A.V. Bondarenko, N.N. Chebotaev. FNT, **32** (6), 746–752. (2006).
36. N.E. Alekseevsky, A.V. Mitin, V.I. Nizhankovskii, et al. SFHT. **2** (10), 40–55. (1989). (Н.Е. Алексеевский, А.В. Митин, В.И. Нижанковский, и др. СФХТ. **2** (10), 40–55. (1989). [In Russian]
37. I.V. Aleksandrov et al. ZhETF Letters. **48** (8), 449–452. (1988). (И.В. Александров и др. Письма в ЖЭТФ. **48** (8), 449–452. (1988)). [In Russian]
38. R.B. Van Dover, L.F. Schneemeyer, J.V. Waszczak, et al. Phys. Rev. B, **39**, 2932–2935. (1989).
39. A. Kebede. Phys. Rev. B, **40**, 4453–4462. (1991).
40. H.B. Radousky. J. Mater. Res., **7** (7), 1917–1955. (1992).
41. V.V. Moshchalkov, I.G. Muttik, N.A. Samarin. FNT. **14** (9), 988–992. (1988) (В.В. Мошchalkов, И.Г. Муттик, Н.А. Самарин. ФНТ. **14** (9), 988–992. (1988)). [In Russian]
42. M.A. Obolenskii, R.V. Vovk, A.V. Bondarenko. Functional Materials, **13** (1), 35–38. (2006).
43. R.V. Vovk, M.A. Obolenskii, A.V. Bondarenko, et al. Acta Physica Polonica A, **111** (1), 129–133. 2007.
44. W.E. Lawrence, S. Doniach. Proceedings of the 12th International Conference on Low Temperature Physics, Kyoto, Japan, 361. (1970).
45. L.G. Aslamazov, A.I. Larkin. FTT, **10** (4), 1104–1111. (1968). (Л.Г. Асламазов, А.И. Ларкин. ФТТ, **10** (4), 1104–1111. (1968)). [In Russian]
46. A.L. Solovyov, H.-U. Habermeyer, T. Haage. FNT, **28** (2), 144–156. (2002).
47. B. Oh, K. Char, A.D. Kent, et al. Phys Rev B, **37**, 7861–7864. (1989).
48. A.A. Varlamov, D.V. Livanov. ZHETF, **98** (2(8)) 584–592. (1990). (А.А. Варламов, Д.В. Ливанов. ЖЭТФ, **98** (2(8)) 584–592. (1990)). [In Russian]
49. L. Reggani, R. Vaglio, A.A. Varlamov. Phys. Rev. B, **44** (17), 9541–9546. (1991).
50. D.D. Prokof'ev, M.P. Volkov, YU.A. Boykov. FTT, **45** (7), 1168–1176. (2003). (Д.Д. Прокофьев, М.П. Волков, Ю.А. Бойков. ФТТ, **45** (7), 1168–1176. (2003)). [In Russian]
51. B.P. Stojkovic, D. Pines. Phys. Rev. B, **55** (13), 8567–8595. (1997).
52. M.V. Sadovsky. UFN, **171** (5), 539–564. (2001) (М.В. Садовский. УФН, **171** (5), 539–564. (2001)).
53. P. Pieri, G.C. Strinati, D. Moroni. Phys. Rev. Lett., **89** (12), 127003(1–4). (2002).
54. R. Griessen. Phys. Rev. B, **36**, 5284. (1987).
55. J. Metzler, T. Weber, W.H. Fietz, et al. Physica C, **214**, 371–376. (1993).
56. V.P. Dyakonov, L. Gladchuk, G.G. Levchenko, G. Shimchak. FTT, **38** (11), 3283–3288. (1996) (В.П. Дьяконов, Л. Гладчук, Г.Г. Левченко, Г. Шимчак. ФТТ, **38** (11), 3283–3288. (1996)). [In Russian]
57. M.A. Obolenskiy, R.V. Vovk, A.V. Bondarenko. FNT, **32** (6), 802–805. (2006) (М.А. Оболенский, Р.В. Вовк, А.В. Бондаренко. ФНТ, **32** (6), 802–805. (2006)).
58. R.P. Gupta, M. Gupta. Phys. Rev. B, **51** (17), 11760–11766. (1995).
59. A.P. Saiko, V.E. Gusakov. FNT, **22** (7), 748–751. (1996) (А.П. Сайко, В.Е. Гусаков. ФНТ, **22** (7), 748–751. (1996)). [In Russian]
60. I.V. Alexandrov, A.F. Goncharov, S.M. Stishov. ZhETF Letters. **47** (7), 357–360. (1988) (И.В. Александров, А.Ф. Гончаров, С.М. Стишов. Письма в ЖЭТФ. **47** (7), 357–360. (1988)). [In Russian]
61. U. Welp, M. Grimsditch, S. Flesher, et al. Phys. Rev. Lett., **69** (9), 2130–2133. (1992).
62. J. Labbe, J. Bok. Europhys. Lett. **3**, 1225. (1987).
63. V.M. Gvozdikov. FNT, **19** (11), 1285–1287. (1993) (В.М. Гвоздилов. ФНТ, **19** (11), 1285–1287. (1993)). [In Russian]
64. D.D. Balla, A.V. Bondarenko, M.A. Obolenskiy, Kh.B. Chashka. Tez. dokl. II-go Vsesoyuznogo simpoziuma “Neodnorodnyye elektronnyye sostoyaniya”, Novosibirsk, **68**. (1987). (Д.Д. Балла, А.В. Бондаренко, М.А. Оболенский, Х.Б. Чашка. Тез. докл. II-го Всесоюзного симпозиума “Неоднородные электронные состояния”, Новосибирск, **68**. (1987)). [In Russian]
65. D.E. Moncton, J.D. Axe, F.J. DiSalvo. Phys. Rev. B, **16**, 801. (1977).
66. H. Suderow, V.G. Tissen, J.P. Brison, et al. Physical Review Letters, **95** (11), 117006. (2005).
67. A. Driessen, R. Griessen, N. Koeman, et al. Phys. Rev. B, **36**, 5602–5607. (1987).
68. M.V. Sadovsky. UFN, **171** (5), 539–564. (2001). (М.В. Садовский. УФН, **171** (5), 539–564. (2001)). [In Russian]
69. J.L. Tallon, C. Bernhard, H. Snaked, et al. Phys. Rev., **51**, 12911. (1995).
70. D. Goldschmidt, A.-K. Klehe, J.S. Schilling, Y. Eckstein. Phys. Rev., **53**, 14631. (1996).
71. S. Sadewasser, J.S. Schilling, A.P. Paulicas, B.M. Veal. Phys. Rev. B., **61** (1), 741–749. (2000).
72. A.A. Abrikosov. Phys. Rev. B., **63**, 104521. (2001).
73. R. Micnas, S. Robaszkiewicz. *High-Tc Superconductivity 1996: Ten Years after the Discovery*, Ed. E. Kaldis, E. Liarokapis, K.A. Miller, Vol.343, (NATO ASI Series E, Kluwer Academic Publishers, The Netherlands, 1997). P.31.
74. M. Krupski, J. Stankowski, S. Przybyl, et al. Physica C, **320**, 120. (1999).
75. R. Micnas, B. Tobbijaszewska. Acta Phys. Polon. B, **32**, 3233. (2001).

76. S. Hikami, A.I. Larkin. *Modern Phys B*, **2**, 693–698. (1988).
77. J.B. Bieri, K. Maki, R.S. Thompson. *Phys. Rev. B*, **44** (9), 4709–4711. (1991).
78. A.N. Bulaevsky. *UFN*, **116** (3), 449–483. (1975) (А.Н. Булаевский. *УФН*, **116** (3), 449–483. (1975)). [In Russian]
79. N.L. Bobrov, A.F. Rybalchenko, M.A. Obolensky. *FNT*, **11** (9), 925. (1985) (Н.Л. Бобров, А.Ф. Рыбальченко, М.А. Оболенский. *ФНТ*, **11** (9), 925. (1985)). [In Russian]
80. L.F. Mattheiss. *Phys.Rev.* **8** (8), 3719–3740. (1973).
81. Kh.B. Chashka, Ye.I. Beletskiy, M.A. Obolenskiy. *FNT*, **17** (7), 833–840. (1991) (Х.Б. Чашка, Е.И. Белецкий, М.А. Оболенский. *ФНТ*, **17** (7), 833–840. (1991)). [In Russian]
82. L.F. Mattheiss *Phys.Rev. Lett.*, **30** (17), 784–787. (1973).
83. J.M.E. Harper, T.H. Geballe, F.J. Di Salvo. *Phys.Rev. B*, **15** (6), 2943–2951. (1977).
84. M.A. Obolensky *Superconductivity in quasi-two-dimensional systems // Thesis for the degree of Doctor of Phys. and Math. Sc.*, Kharkov, 1993. (М.А. Оболенский *Сверхпроводимость в квазидвумерных системах // диссертация на соискание ученой степени д. физ.-мат. наук, Харьков, 1993*). [In Russian]
85. S. Sugai. *Phys. Stat-Solidi*, **B129** (1), 14–39. (1985).
86. E.A. Antonova, C.A. Medvedev, Yu.I. Shebalin. *ZhETF*. **57** (2), 329–337. (1970) (Е.А. Антонова, С.А. Медведев, Ю.И. Шебалин. *ЖЭТФ*. **57** (2), 329–337. (1970)). [In Russian]
87. D. Jerome, A.J. Grant, A.D. Yoffe. *Solid State Commun.*, **9**, 2183–2185. (1971).
88. D. Jerome, C. Berthier, P. Moline. *Solid State Commun.*, **18**, 1935–1939. (1976).
89. D.D. Balla, L.S. Golovko, V.I. Kolesnikov, et al. *FNT*, **4** (5), 617–621. (1978) (Д.Д. Балла, Л.С. Головки, В.И. Колесников, и др. *ФНТ*, **4** (5), 617–621. (1978)). [In Russian]
90. D.D. Balla, A.A. Mamalui, M.A. Obolensky, et al. *FNT*, **5** (9), 1080–1082. (1979) (Д.Д. Балла, А.А. Мамалуй, М.А. Оболенский, и др. *ФНТ*, **5** (9), 1080–1082. (1979)). [In Russian]
91. T. Sambongi. *J. Low Temp. Phys.*, **18** (1-2), 139–146. (1975).
92. M.A. Obolenskiy, Kh.B. Chashka, V.I. Beletskiy, V.M. Gvozdikov. *FNT*, **15** (9), 984–988. (1989) (М.А. Оболенский, Х.Б. Чашка, В.И. Белецкий, В.М. Гвоздики. *ФНТ*, **15** (9), 984–988. (1989)). [In Russian]
93. D.D. Balla, A.V. Bondarenko, M.A. Obolenskiy, Kh.B. Chashka *Tez. dokl. II-go Vsesoyuznogo simpoziuma “Neodnorodnyye elektronnyye sostoyaniya”*, Novosibirsk, **68**. (1987). (Д.Д. Балла, А.В. Бондаренко, М.А. Оболенский, Х.Б. Чашка *Тез. докл. II-го Всесоюзного симпозиума “Неоднородные электронные состояния”*, Новосибирск, **19**. (1987)). [In Russian]